Clinical Research in Cardiology (2019) 108:691–702
https://doi.org/10.1007/s00392-018-1398-9

ORIGINAL PAPER

MicroRNA-214 promotes the calcification of human aortic valve interstitial cells through the acceleration of inflammatory reactions with activated MyD88/NF-κB signaling

Dongdong Zheng[1] · Yue Zang[1] · Haixia Xu[1] · Yan Wang[1] · Xiang Cao[2] · Teng Wang[1] · Min Pan[1] · Jiahai Shi[2] · Xiaofei Li[1]

Received: 26 April 2018 / Accepted: 28 November 2018 / Published online: 5 December 2018

Abstract

Calcific aortic valve disease (CAVD) is a complex active process involving in endothelial injury, lipid infiltration, chronic inflammation, matrix remodeling, cell differentiation, progressive bone formation, and new angiogenesis. The excess inflammatory responses induced by aortic valve interstitial cells (AVICs) are one of the common pathogeneses of this disease. Although many microRNAs (miRs) have been identified to play crucial roles in the calcification process of the aortic valve, numerous miRs are still waiting to be explored. In this study, we explored the functional role of miR-214 in the inflammatory reaction and calcification of human AVICs and its underlying molecular mechanism. Alizarin red staining was used to determine the number of calcified nodules. The protein levels of ICAM-1, IL-6, IL-8, and MCP-1 detected by enzyme-linked immunosorbent assay (ELISA) were used to assess the inflammatory reaction of AVICs; expression levels of RUNX2, Msx2, and BMP2 were used to evaluate AVICs osteoblast differentiation. Results showed that the expression levels of TLR4, MyD88, NF-κB, and miR-214 were up-regulated in the blood and aortic valve tissue samples of patients with CAVD when compared with normal individuals. Knockdown of miR-214 in AVICs inhibited the secretion of IL-6, IL-8, ICAM-1, and MCP-1, while this effect was repressed when lipopolysaccharide (LPS) was added to AVICs. LPS also enhanced the effects of miR-214 in promoting the secretion of pro-inflammatory factors. Besides, up-regulation of miR-214 promoted the protein expression of MyD88 and NF-κB but had no influence on TLR4, and miR-214 could directly combine with MyD88 protein. Up-regulation of MyD88 facilitated the secretion of pro-inflammatory factors and increased calcified nodules number and accelerated the expression of RUNX2, Msx2, and BMP2. Moreover, promotion of the expressions of pro-inflammatory factors and "osteoblast-like" cell markers induced by miR-214 overexpression was abolished when MyD88 was down-regulated in AVICs. In conclusion, this study revealed that miR-214 promoted calcification by facilitating inflammatory reaction through MyD88/NF-κB signaling pathway in AVICs.

Keywords MiR-214 · Calcification · Inflammatory response · MyD88 · NF-κB · Aortic valve interstitial cells

Introduction

Calcific aortic valve disease (CAVD), a common cardiovascular disease and a significant cause of morbidity in the elderly, is present in almost 30% of adults over 65 years of age and in 40–50% in those over 75 years [1, 2]. CAVD is a complex active process involving in endothelial injury, lipid infiltration, chronic inflammation, matrix remodeling, cell differentiation, progressive bone formation, and new angiogenesis. The prevalence of CAVD is increasing worldwide due to lengthening lifespans. However, the pathogenic mechanism responsible for CAVD remains largely unclear, and to date, no pharmacological

Dongdong Zheng and Yue Zang contributed equally to this work.

✉ Xiaofei Li
lixiaofeint1991@163.com

[1] Department of Cardiology, Affiliated Hospital of Nantong University, No. 20, Xisi Road, Chongchuan District, Nantong 226001, Jiangsu, China

[2] Department of Cardio-Thoracic Surgery, Affiliated Hospital of Nantong University, Nantong 226001, Jiangsu, China

intervention has been found that delays or halts its progression [3]. A thorough understanding of the mechanisms behind CAVD development and progression is required to identify potential targets for pharmacological intervention.

CAVD is pathologically characterized by changes including chronic inflammation with leukocytic infiltration that includes macrophages, T lymphocytes, and mast cells [4, 5]. And inflammatory infiltrates is closely associated with osteogenic metaplastic changes in the aortic valve tissues [6]. In this regard, pro-inflammatory cytokines, such as tumor necrosis factor-α (TNF-α), monocyte chemotactic protein-1 (MCP-1), interleukin (IL)-1β, IL-6, and IL-8 are believed to play a role in exacerbating inflammation-mediated valvular calcification [7].

Aortic valve interstitial cells (AVICs), the main cellular component of the aortic valve, play an important role in the pathogenesis of CAVD [8]. Cumulative evidence has demonstrated that AVICs can secrete intercellular adhesion molecule-1 (ICAM-1), IL-8, and MCP-1 when stimulated with Toll-like receptor 2 (TLR2) and TLR4 agonists [9, 10]. Additionally, AVICs differentiate into "osteoblast-like" cells characterized by increased alkaline phosphatase (ALP) activity and greater levels of runt-related transcription factor 2 (RUNX2) following stimulation by cytokines and TLR2/4 agonists [11–13], indicating that TLR-related signaling pathway such as TLR4/MyD88/NF-κB plays an important role in aortic valve calcification through promoting AVIC osteogenic differentiation.

MicroRNAs (miRNAs) are a class of small noncoding, single-stranded RNAs with 19–25 nucleotides that promote the degradation of messenger RNAs (mRNAs) or inhibit their translation [14]. They regulate gene expression negatively at the post-transcriptional level by binding to imperfect complementary sites at the 3′ untranslated region (UTR) of their target mRNA transcripts [15]. The binding of miRNAs to their target mRNAs leads to translational repression or decreases the stability of the mRNA. MiRNAs regulate various biological processes, including cell differentiation, cell proliferation, apoptosis, drug resistance, and fat metabolism [16]. Recently, lots of reports indicate that a group of miRNAs is involved in the differentiation of mesenchymal cells or myofibroblasts into osteoblastic phenotype and subsequent heterotopic ossification. Fang et al. [17] demonstrated that miR-29b promoted the calcification of human AVICs via inhibiting TGF-β3 through activation of wnt3/β-catenin/Smad3 signaling. MiR-214 was reported to inhibit human mesenchymal stem cells differentiating into osteoblasts through targeting β-catenin [18]. However, the role of miR-214 in CAVD has not yet been completely reported.

Overall, the objective of the present study is to explore the effects of miR-214 in the osteogenic differentiation of human AVICs, as well as to identify the underlying molecular mechanism in hopes of finding a new target for early intervention of CAVD.

Materials and methods

Materials

Small interference (si) RNAs targeting human myeloid differentiation factor 88 (MyD88), overexpressed vector-MyD88 and their controls were purchased from OriGene (MA, USA). The transfection reagents were purchased from Santa Cruz Biotechnology, Inc. (California, USA). Antibodies against TLR4, MyD88, NF-κB, ICAM-1, RUNX2, msh homeobox 2 (Msx2), bone morphogenetic protein 2 (BMP2), osterix, bone sialoprotein and glyceraldehyde 3-phosphate dehydrogenase (GAPDH) were purchased from Abcam (Burlingame, California, USA). Medium 199 was purchased from Lonza (Walkersville, Maryland, USA). Cytokine ELISA kits were purchased from R&D Systems (Minneapolis, Minnesota, USA). The NF-κB p65 ELISA-based transcription factor assay kit (TransAM™ assay) was obtained from Active Motif (Carlsbad, CA, USA). LPS (*E. coli* 0111:B4). Other chemicals and reagents were purchased from Sigma-Aldrich Chemical Co (St Louis, Missouri, USA).

Human aortic valve tissue and blood samples

This work was approved by the ethics committee of the Affiliated Hospital of Nantong University. Written informed consent was obtained from every patient. Patients included were selected during cardiac valve replacement surgery at the department of cardiovascular surgery in affiliated Hospital of Nantong University. Patients with malignancies, poor renal or hepatic function, acute and chronic lung disease, diabetes, cerebrovascular disease, autoimmune disease, rheumatic heart disease, and infective endocarditis were eliminated from this study. Human whole calcified aortic valve tissue and blood samples were obtained from patients with aortic stenosis ($n=8$); control samples (no calcified aortic valve tissue and blood samples) were taken from age-matched patients with aortic insufficiency ($n=8$).

Immunohistochemistry

A slicing machine was used to cut human aortic valve tissue specimens into 4-μm-thick paraffin sections. Then, a routine three-step immunohistochemical staining protocol was conducted: sectioning, dewaxing, and hydrating tissues; incubation with 3% H_2O_2 at room temperature for 10 min; antigen retrieval with Tris–EDTA; sealing with 5% goat serum [diluted in phosphate-buffered saline (PBS)];

incubation overnight at 4 °C with primary antibody against TLR4, NF-κB, and MyD88; and as the last step incubation with secondary antibody and rinsing with PBS. Chromogen 3,3′-diaminobenzidine tetrachloride (Serva, Heidelberg, Germany) was used as a substrate, and the cell nucleus was dyed with Harris's hematoxylin solution.

Cell isolation and culture

Normal aortic valve leaflets were collected from the hearts of 8 patients (4 males and 4 females; mean age, 60.5 ± 7.5 years) that had been explanted for the purpose of heart transplantation due to advanced cardiomyopathy. All patients gave informed consent for the use of their aortic valves for this study.

AVICs were isolated and cultured using a previously described method [19] with modification [20]. Briefly, valve leaflets were subjected to sequential digestions with collagenase, and cells were collected by centrifugation. Cells were cultured in M199 growth medium containing penicillin G, streptomycin, amphotericin B, and 10% fetal bovine serum (FBS). Cells of passages 4–6 were used for our study. Cells were subcultured on plates and treated when they reached 80–90% confluence. If AVICs differentiate into "osteoblast-like" cells, the activation of ALP and ectopic calcification will be promoted with the high expression levels of markers of osteoblastogenesis, such as RUNX, BMP2, Msx, osterix, and bone sialoprotein.

To determine the effect of TLR stimulation on inflammatory mediator production, cells were treated with TLR4 agonist LPS (0.1 μg/mL).

Cell transfection

Cells in the miR-214 mimic group were transfected with a miR-214 mimic (5′-ACA GGU AGC UGA ACA CUG GGU U-3′; Shanghai GenePharma Co., Ltd., Shanghai, China). Cells in miR-214 inhibitor group were transfected with mirVana™ miRNA inhibitor (5′-UCA CAG UGC UCA UCA UGA AUA A-3′; Shanghai GenePharma Co., Ltd.). AVICs were transfected with lipofectamine 2000 (Invitrogen; Thermo Fisher Scientific, Inc., Waltham, Massachusetts, USA) when cell density reached 40–60%, according to the manufacturer's instructions. Lipofectamine 2000 (5 μL), miR-214 mimic, miR-214 inhibitor, si-MyD88, and vector-MyD88 along with any controls (100 pmol; final concentration, 50 nM) were, respectively, diluted in 250 μL serum-free medium Opti-MEM (Gibco; Thermo Fisher Scientific, Inc.), gently mixed until evenly distributed within the mixture, and incubated for 5 min at room temperature. The diluted si-MyD88, vector-MyD88, miR-214 mimic, and miR-214 inhibitor and controls were then evenly mixed with the diluted lipofectamine 2000. The mixture was added into the cell-containing well following incubation for 20 min at room temperature and gently mixed until even. The transfected cells were placed in a 5% CO_2 incubator at 37 °C; the medium was replaced with the complete medium after 6 h incubation at 37 °C. The transfected cells were incubated at 37 °C for 24–48 h for subsequent experiments.

Real-time PCR detection (RT-PCR)

Total RNA was extracted from cells by a Trizol reagent (Invitrogen, Carlsbad, CA, USA). Total RNA (2 μg) was reverse-transcribed to complementary DNA (cDNA) using avian myeloblastosis virus transcriptase and random primers (Takara; Dalian, China). The oligonucleotide primers for PCR were based on GenBank sequences. RT-PCR amplification of the cDNA was performed in the 20-μL reaction system with the SYBR Premix Ex Taq™ II kit (Takara, Dalian, China) and was carried out using an ABI 7500 real-time PCR System (Carlsbad, CA, USA). Data from RT-PCR were analyzed by the ΔC_t method [21]. β-Actin was used as the internal control. U6 snRNA Normalization RT-PCR Quantitation (GenePharma) was used to check miR-214. The primers were are as follows: β-actin (F): TGC GTG ACA TTA AGG AGA AG, (R): GCT CGTAGC TCT TCT CCA; TLR4 (F): GGTGCCTCCATTTCAGCTCT; (R): ACTGCCAGGTCTGAGCAATC; NF-κB p65 (F): TGG CCCCTATGTGGAGATCA, (R): GTATCTGTGCTCCTC TCGCC; MyD88 (F): GTCTCCTCCACATCCTCCCT, (R): CGGCACCAATGCTGGGTC; RUNX2 (F): CATGTCCCT CGGTATGTCCG, (R): ACTCTGGCTTTGGGAAGAGC; Msx2 (F): CTGGTGAAGCCCTTCGAGAC, (R): AGGGCT CATATGTCTTGGCG; BMP2 (F): GCTGTCTTCTAGCGT TGCTG, (R): CTGTTTCAGGCCGAACATGC; H-miR-214 (F): GTACAGCAGGCACAGAC; (R): GTGCAGGGTCCG AGGT; H-U6s (F): ATT GGA ACG ATA CAG AGA AGA TT; (R): GGA ACG CTT CAC GAA TTT G.

Western blot analysis

Cells and tissues were extracted in a lysis buffer containing 50 mM sodium chloride (NaCl), 1 mM ethylene glycol tetraacetic acid, 0.1% sodium dodecyl sulfate (SDS), 1 mM sodium fluoride, 1 mM sodium orthovanadate, 1 mg/mL aprotinin, and 1 mg/mL leupeptin in 10 mM Tris buffer (pH 7.4) and proteinase inhibitor (1 mM *n*-phenylmethanesulfonyl fluoride). After quantification with the BCA method (Thermo Fisher Scientific), equal amounts of protein samples were separated by a 10% SDS–polyacrylamide gel and transferred to nitrocellulose membranes (Millipore). The membranes were then incubated overnight with monoclonal antibodies against TLR4 (no. ab13556), MyD88 (no. ab2064), NF-κB (no. ab16502), ICAM-1 (no. ab20), RUNX2 (no. ab23981), Msx2 (no. ab223692), BMP2 (no. ab14933),

and GAPDH (no. ab8245), respectively. The membrane was washed three times with Tris-buffered saline–Tween 20 (TBST) and incubated with secondary antibodies (Bioworld; Louis Park, Minnesota, USA) at 37 °C for 1 h. The immune complexes were examined by ECL detection (Millipore). ImageJ software (National Institutes of Health, Bethesda, Maryland, USA) was used to quantify western blot bands after background subtraction.

RNA pull-down assay

The association between miR-214 and MyD88 or NF-κB protein were analyzed by RNA pull-down assay using Pierce™ Magnetic RNA-Protein Pull-Down Kit (Thermo, MA, USA), according to the manufactures' instructions. Briefly, miRNA-214 was labeled with desthiobiotinylated cytidine bisphosphate and T4 RNA ligase, then the labeled RNA was incubated with streptavidin magnetic beads for 15–30 min at room temperature with agitation. Then placed the tube into a magnetic stand to collect the beads against the side of the tube and removed the supernatant. Subsequently, beads were washed twice in 20 mM Tris (pH 7.5), and 100 µL of 1× protein–RNA and 40 µg of AVICs protein extract were added into the beads and incubated for 45 min at 4 °C, followed by being washed with wash buffer for three times and being eluted after 15 min of incubation with 50 µL biotin elution buffer at 37 °C. Then the eluted samples and supernatant were collected for western blot analysis with antibodies against MyD88 (no. ab2064) and NF-κB (no. ab16502) referring to the above procedure.

ALP activity detection

ALP activity was measured to quantify the osteoblast differentiation of AVICs. Briefly, the AVICs were seeded into the 5-cm^2 dish and given different treatment: inhibitor-NC, inhibitor, mimic-NC and mimic. The cells were then harvested and lysed with 1% Triton X-100 after 7 days of the treatments. The ALP activity of the cells was assessed at 405 nm using a *p*-nitrophenol phosphate substrate kit (Sigma-Aldrich, MO, USA). The ALP values (units/ng protein) were normalized to those of proteins using a Bio-Rad DC protein assay (Bio-Rad).

Duolink assay

Duolink experiments were performed to detect close proximity between MyD88 and NF-κB. After incubated with antibodies against MyD88 and NF-κB overnight at 4 °C, the cells were incubated with PLA probes from the Duolink kit (Sigma-Aldrich, MO, USA). The remainder of the protocol was conducted according to the manufacturer's recommendations, and an orange (555 nm wavelength) detection kit was used. Hybridization between two PLA plus and minus probes leads to a fluorescent signal and occurs only when the distance between two antigens is less than 40 nm.

Co-immunoprecipitation analysis (co-IP)

The co-IP procedure was performed to evaluate the interaction between NF-κB protein and MyD88 protein. Briefly, cells were lysed with lysis buffer (50 mM Tris–HCl, pH 7.5, 200 mM NaCl, 0.5% Nonidet P40, protease inhibitor cocktail) at 4 °C for 30 min. After centrifuged at 15,000 rpm for 10 min, the supernatant was subjected to IP with 1 µg antibody against MyD88 (no. ab2064) overnight, followed by incubated with 10 µL protein A beads at 4°X for 2 h, then the immune complex was detected by western blot with NF-κB (no. ab16502) antibody referring to the above procedure.

Alizarin red staining

For alizarin red staining, the cells were washed in distilled water and then exposed to freshly prepared 2% alizarin red s (pH to 4.1–4.3, Sigma) for 5 min (red/orange = positive staining) [22]. Digital images were taken on a Zeiss Axio Imager upright microscope (Oberkochen, Germany) for the transmitted light bright field. Calcification of AVICs was assessed using standard protocols for alizarin red staining. Quantification was performed using Image-Pro Plus software (Media Cybernetics; Rockville, MD, USA).

NF-κB transcription factor assay

Aortic valve interstitial cells were seeded into a 6-well plate and grown overnight at 37 °C in 5% CO_2. After transfection with inhibitor-miR-214, mimic-miR-214, and their control vectors for 48 h, nuclear proteins were extracted using the Active Motif Nuclear Extract Protocol (Active Motif) and the total protein concentration of the lysates was determined using the BCA Protein Assay kit (Thermo Fisher Scientific). Activation of the NF-κB p65 subunit in 5 µg of nuclear extracts was determined using an NF-κB p65 ELISA-based transcription factor assay kit (TransAM™ assay) according to the manufacturer's instructions. The NF-κB detecting antibody recognized an epitope on p65 that was accessible only when NF-κB was activated. The colorimetric reading at 450 nm was determined in a microplate reader (molecular devices). The positive-control Jurkat nuclear extract provided with the kit was used to assess assay specificity.

Enzyme-linked immunosorbent assay (ELISA)

The levels of IL-6, IL-8, and MCP-1 in culture supernatants were determined using ELISA kits following the manufacturer's instructions.

Statistical analysis

Data are presented as the mean ± standard deviation (SD). Statistical analysis was performed using SPSS 23.0 (SPSS Inc.; Chicago, IL, USA). Student's *t* test was used for comparison between two groups. Analysis of variance (ANOVA) with the post hoc Bonferroni/Dunn test was used to analyze differences among multiple groups. The nonparametric Mann–Whitney *U* test was performed to confirm the difference of the 2-group comparison. Differences were confirmed for multiple group comparisons using the nonparametric Kruskal–Wallis test. Statistical significance was defined as $P < 0.05$.

Results

Expression of miR-214, TLR4, MyD88, and NF-κB in CAVD patients

To explore the function of miR-214 in the occurrence and development of CAVD and its underlying mechanism, we first ascertained the expression patterns of miR-214, TLR4, MyD88, and NF-κB in the blood and aortic valve tissue samples of patients with calcified aortic stenosis ($n = 8$) or the age-matched patients with aortic insufficiency ($n = 8$). Immunohistochemical staining and western blot tests showed the expression levels of TLR4, MyD88, and NF-κB proteins were all elevated in the aortic valve tissues of patients with calcified aortic stenosis when compared with the non-cardiac tissues (Fig. 1a, c). RT-PCR showed that the level of miR-214 was also increased in the blood and aortic valve tissue samples of calcified aortic stenosis patients, as well as the mRNA levels of TLR4, MyD88, and NF-κB

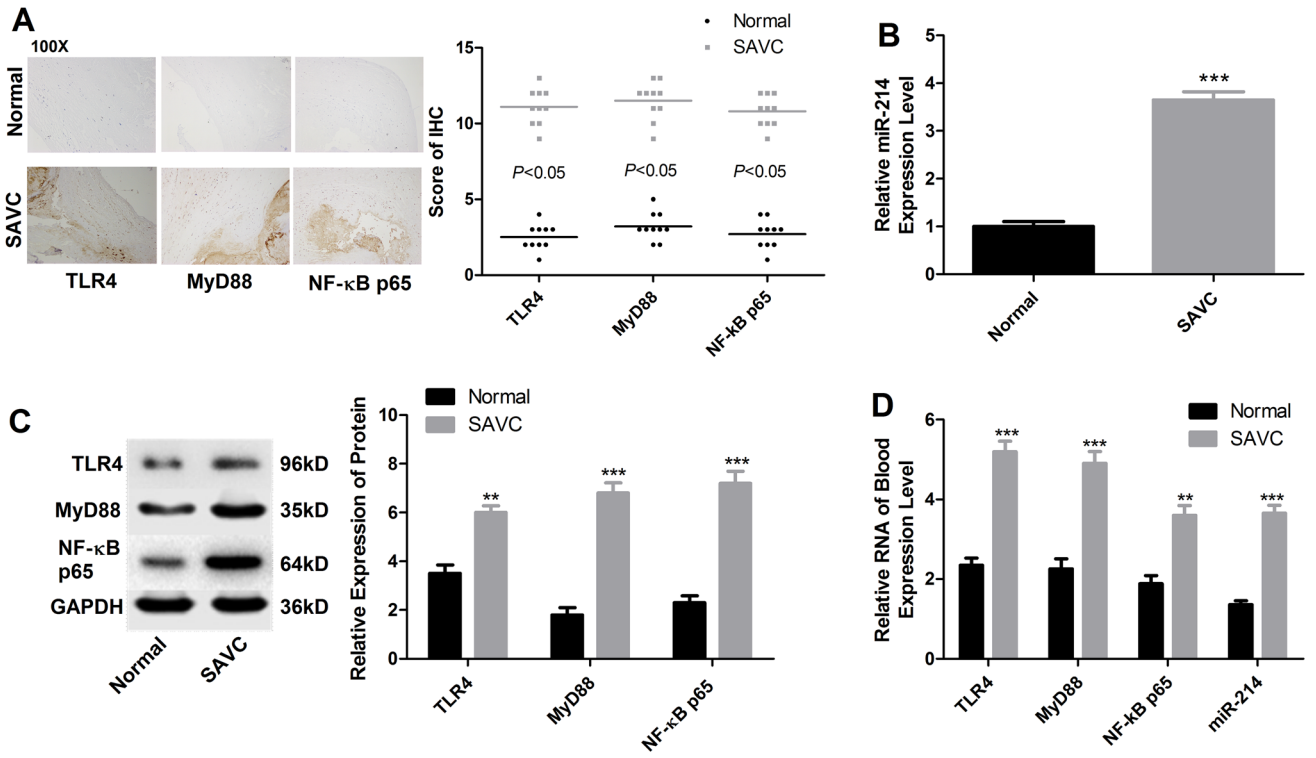

Fig. 1 Detection of the expression of miR-214, TLR4, MyD88, and NF-κB in CAVD patients. **a** Immunohistochemical staining analysis of the protein levels of TLR4, MyD88, and NF-κB in the aortic valve tissue specimens from patients with calcified aortic stenosis ($n = 8$) or the age-matched patients with aortic insufficiency ($n = 8$). Magnification: ×100. **b** RT-PCR analysis of the expression of miR-214 in the aortic valve tissue specimens from patients with calcified aortic stenosis and the age-matched patients who had aortic insufficiency. **c** Western blot tests were performed to assess the protein levels of TLR4, MyD88, and NF-κB in the aortic valve tissue specimens from patients with calcified aortic stenosis ($n = 8$) or the age-matched patients with aortic insufficiency ($n = 8$). GAPDH was used to normalize the expression of proteins. **d** RT-PCR analysis of the levels of miR-214, TLR4, MyD88, and NF-κB in the blood samples from calcified aortic stenosis ($n = 8$) or the age-matched patients with aortic insufficiency ($n = 8$). Error bars represent the mean ± SD of at least three independent experiments. (*P<0.05, **P<0.01, ***P<0.001, CAVD group vs normal group)

(Fig. 1b, d). These results indicated that miR-214, TLR4, MyD88, and NF-κB were highly expressed in the blood and tissue samples of CAVD patients, suggesting that these molecules might play a role in the pathogenesis of CAVD.

LPS reverses the down-regulated expression of IL-6, IL-8, MCP-1, and ICAM-1 induced by miR-214 down-regulation

Then we explored the function of miR-214 in the inflammatory reaction of AVICs. Figure 2a shows the transfected efficiency of the inhibitor and mimic of miR-214. The level of miR-214 was reduced markedly when AVICs were transfected with inhibitor-miR-214, while miR-214 expression was increased when AVICs were transfected with mimic-miR-214 (Fig. 2a). ELISA showed that inhibitor-miR-214 reduced the protein levels of IL-6, IL-8, and MCP-1, whereas these results were reversed when adding LPS, agonist of TLR4, at the same time of miR-214 down-regulation (Fig. 2b). Additionally, up-regulation of miR-214 by transfection of mimic-miR-214 increased the protein levels of IL-6, IL-8, and MCP-1 in AVICs, and this effect was enhanced by LPS (Fig. 2c). Also, we evaluated the protein level of ICAM-1 in different treated AVICs. Down-regulation of miR-214 decreased the expression of ICAM-1 and up-regulation of miR-214 increased ICAM-1 expression, while LPS reinforced ICAM-1 expression regardless of miR-214 up-regulation or down-regulation (Fig. 2d). These results suggest that both LPS and miR-214 enhanced the expression of IL-6, IL-8, MCP-1, and ICAM-1.

Up-regulation of miR-214 accelerates AVICs calcification and activates MyD88/NF-κB signaling pathway

Then, we explored the effect of miR-214 on the activation of TLR4/MyD88/NF-κB signaling pathway. Up-regulation of miR-214 increased the protein expression of MyD88 and NF-κB, while down-regulation of miR-214 showed the opposite results with no obvious influence in TLR4

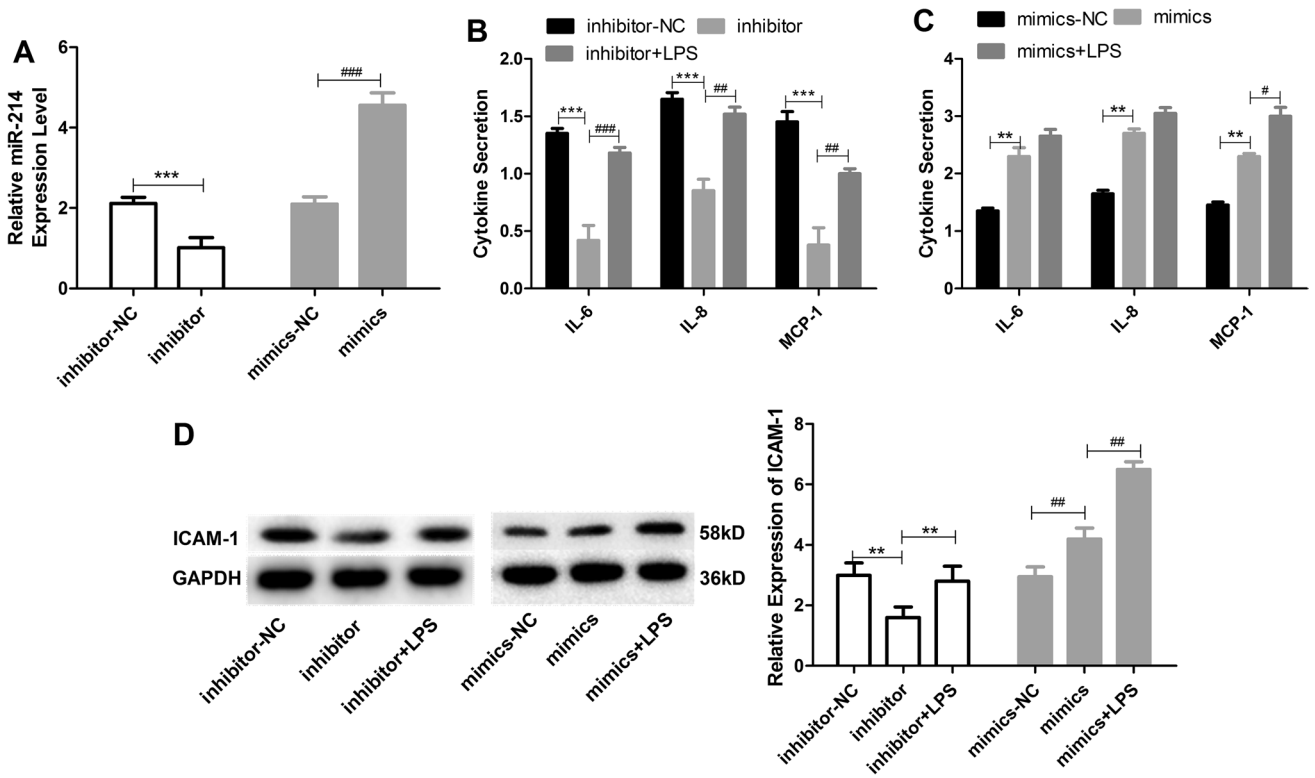

Fig. 2 Detection of the protein levels of IL-6, IL-8, MCP-1, and ICAM-1 in AVICs with different groups. **a** RT-PCR analysis of the expression of miR-214 24 h after AVICs transfected with inhibitor-miR-214, mimic-miR-214, or their control vectors. **b** ELISA was used to analyze the protein levels of IL-6, IL-8, and MCP-1 in the supernatant samples of AVICs with different treatments: inhibitor-NC (48 h), inhibitor-miR-214 (48 h), inhibitor-miR-214 (48 h) + LPS (0.2 μg/mL, 12 h). **c** ELISA was used to analyze the protein levels of IL-6, IL-8, and MCP-1 in the supernatant samples of AVICs with different treatments: mimic-NC (48 h), mimic-miR-214 (48 h), mimic-miR-214 (48 h) + LPS (0.2 μg/mL, 12 h). **d** Western blot tests were performed to detect the expression of ICAM-1 in different treated AVICs: inhibitor-NC (48 h), inhibitor-miR-214 (48 h), inhibitor-miR-214 (48 h) + LPS (0.2 μg/mL, 12 h), mimic-NC (48 h), mimic-miR-214 (48 h) and mimic-miR-214 (48 h) + LPS (0.2 μg/mL, 12 h). Error bars represent the mean ± SD of at least three independent experiments. (*,$^{\#}P<0.05$, **,$^{\#\#}P<0.01$, ***,$^{\#\#\#}P<0.001$)

expression (Fig. 3a). Besides, the DNA-binding activity of NF-κB p65 was significantly increased when AVICs were transfected with mimic-miR-214 and vice versa (Fig. 3b). Then, we explored the function of miR-214 in the calcification of AVICs through detecting ALP activity and alizarin red staining. And results demonstrated that upregulation of miR-214 significantly increased ALP activity (Fig. 3c) and the area of calcified nodules (Fig. 3d), and vice versa. Similarly, both the protein and mRNA levels of RUNX2, Msx2, and BMP2 were elevated in the mimic-miR-214 group, while these results were reversed in the inhibitor-miR-214 group (Fig. 3e, f). These data indicated that overexpression of miR-214 promoted the calcification of AVICs and activated the MyD88/NF-κB signaling pathway.

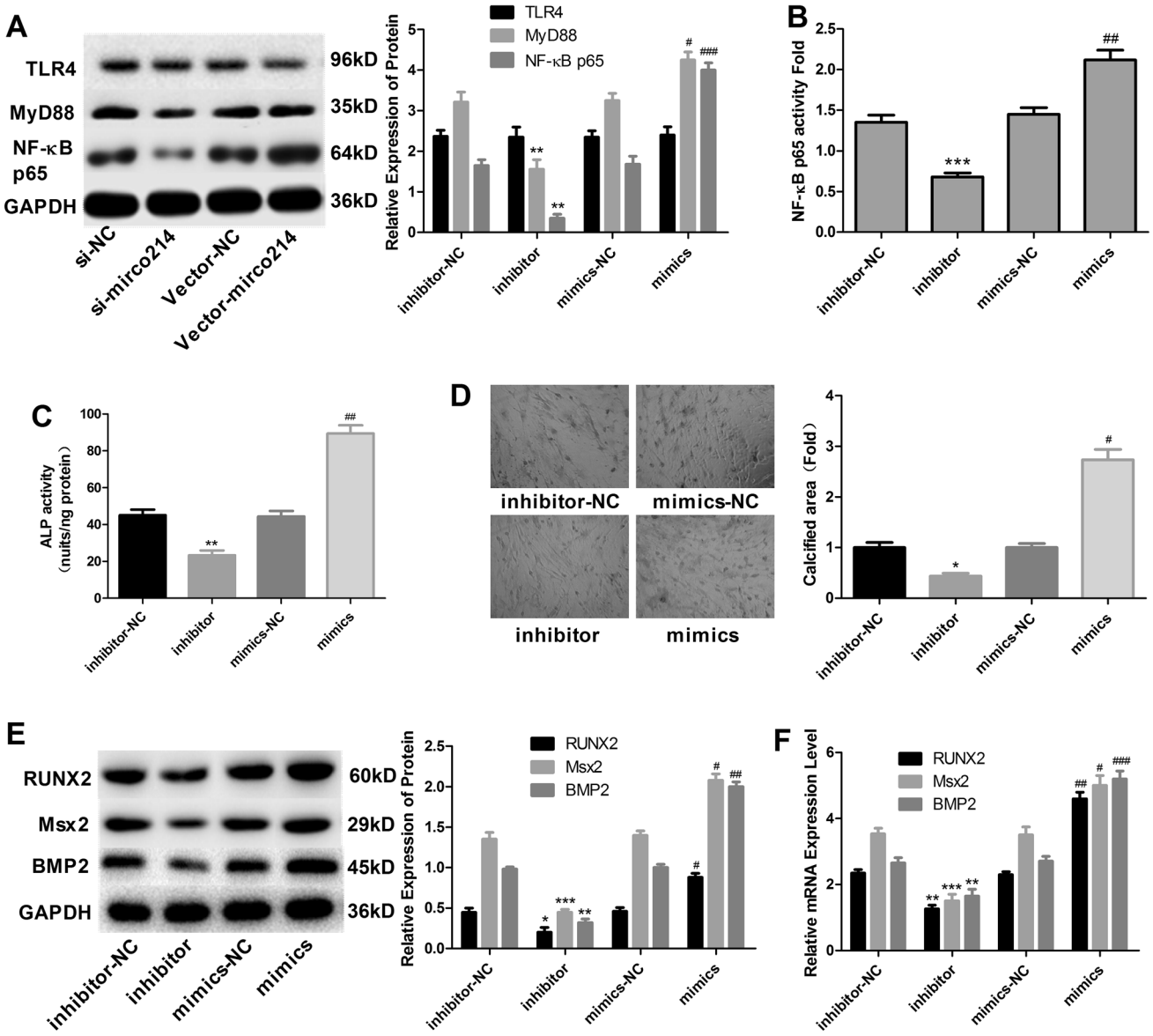

Fig. 3 Determination of the effects of miR-214 on the calcification of AVICs and its related signaling pathway. After AVICs were transfected with inhibitor-NC, inhibitor-miR-214, mimic-NC, and mimic-miR-214., then **a** western blot tests were performed to detect the protein levels of TLR4, MyD88, and NF-κB. **b** For TransAM assays, nuclear extracts of AVICs were prepared and the DNA-binding activity of p65 was measured using an ELISA-based TransAM kit. **c** ALP activity of AVICs after 7 days of the transfection. **d** Calcified nodules were apparent with the use of alizarin red staining. Magnification: ×100. **e** Western blot tests were performed to detect the protein levels of RUNX2, Msx2, and BMP2. **f** RT-PCR analysis of mRNA levels of RUNX2, Msx2, and BMP2 after 24 h AVICs were transfected with inhibitor-NC, inhibitor-miR-214, mimic-NC, and mimic-miR-214. Error bars represent the mean ± SD of at least three independent experiments. (*$P < 0.05$, **$P < 0.01$, ***$P < 0.001$, inhibitor-miR-214 vs inhibitor-NC; $^{\#}P < 0.05$, $^{\#\#}P < 0.01$, $^{\#\#\#}P < 0.001$, mimic-miR-214 vs mimic-NC)

MiR-214 interacts with the MyD88 protein in AVICs

As miR-214 could activate MyD88/NF-κB signaling (Fig. 3a, b), we next determined the interaction between miR-214 and MyD88 and NF-κB proteins. RNA pull-down assay using anti-NF-κB and MyD88 antibodies determined that miR-214 could directly combine with MyD88 protein but not NF-κB protein (Fig. 4a). Furthermore, we carried out Duolink and co-IP assays to evaluate the interaction between MyD88 and NF-κB proteins. Results demonstrated that there was co-location in nuclear of MyD88 and NF-κB proteins (Fig. 4c) and these two proteins could direct or indirect bind to each other (Fig. 4b). Together, these result revealed that there was a close relationship between miR-214 and MyD88/NF-κB signaling in AVICs.

MiR-214 accelerates AVICs calcification through the activation of MyD88/NF-κB signaling pathway

Finally, we investigated the effects of MyD88/NF-κB in the calcification of AVICs with or without the presence of miR-214. Vector-MyD88 and siRNAs-MyD88 were used to up-regulate and down-regulate the expression of MyD88 in AVICs. Figure 5a shows the transfected efficiency of them, and si-3 showed the highest knockdown efficiency of MyD88 and was accordingly chosen for the next study. Up-regulation of MyD88 promoted both the mRNA and protein expression of NF-κB (Fig. 5b) and increased the levels of pro-inflammatory cytokines such as IL-6, IL-8, and MCP-1 (Fig. 5c). Besides, both the protein and mRNA levels of RUNX2, Msx2, and BMP2 were increased with up-regulation of MyD88 (Fig. 5d, e), as well as the increased ALP activity and the area of calcified nodules (Fig. 5f, g); the reverse was also true when knockdown of MyD88 in AVICs (Fig. 5b–g).

Overexpression of miR-214 increased the expressions of NF-κB (Fig. 6a), IL-8, MCP-1, ICAM-1 (Fig. 6b), and osterix, bone sialoprotein, RUNX2, Msx2 and BMP2 (Fig. 6c), enhanced ALP activity (Fig. 6d) and area of calcified nodules (Fig. 6e), whereas these effects mediated by miR-214 up-regulation were abolished when MyD88 was down-regulated in AVIVs (Fig. 6). Taken together, these results suggested that miR-214 accelerated the inflammatory process and calcification of AVICs through activation of the MyD88/NF-κB signaling pathway.

Discussion

CAVD is a complex process [23] with endothelial damage, lipid deposition, inflammatory cell accumulation, and resultant production of pro-inflammatory mediators [24]. The inflammatory responses and osteogenic differentiation of AVICs account for the main pathogenesis of this disease [25]. In the present study, we clarified that overexpression of miR-214 promoted the production of pro-inflammatory mediators such as ICAM-1, IL-6, IL-8, and MCP-1, and accelerated the osteogenic differentiation of AVICs through activation of MyD88/NF-κB signaling. These findings illustrate that miR-214 exerts pro-inflammatory roles in human AVICs and miR-214 inhibition has the potential to suppress inflammatory processes and repress the calcification of AVICs, providing a promising target for CAVD treatment.

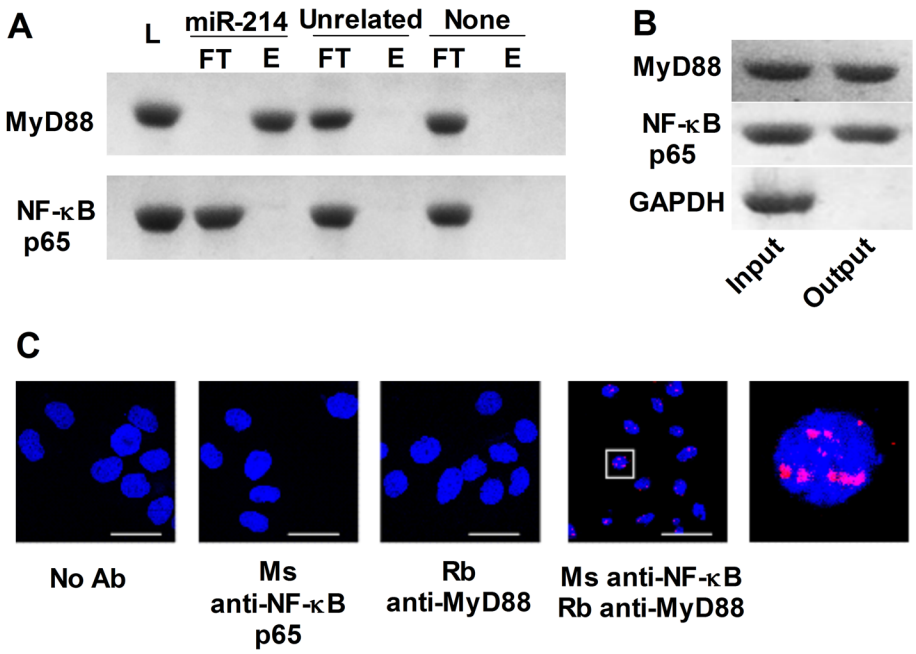

Fig. 4 miR-214 could combine with MyD88 protein. **a** RNA pull-down assay was performed to determine if miR-214 could directly bind to MyD88 protein (*L* lysate load; *FT* flow-through; *E* eluate). **b** Co-IP assay was performed to evaluate the interaction between MyD88 and NF-κB proteins in AVICs. **c** Duolink assay was used to assess the co-subcellular location of MyD88 and NF-κB proteins

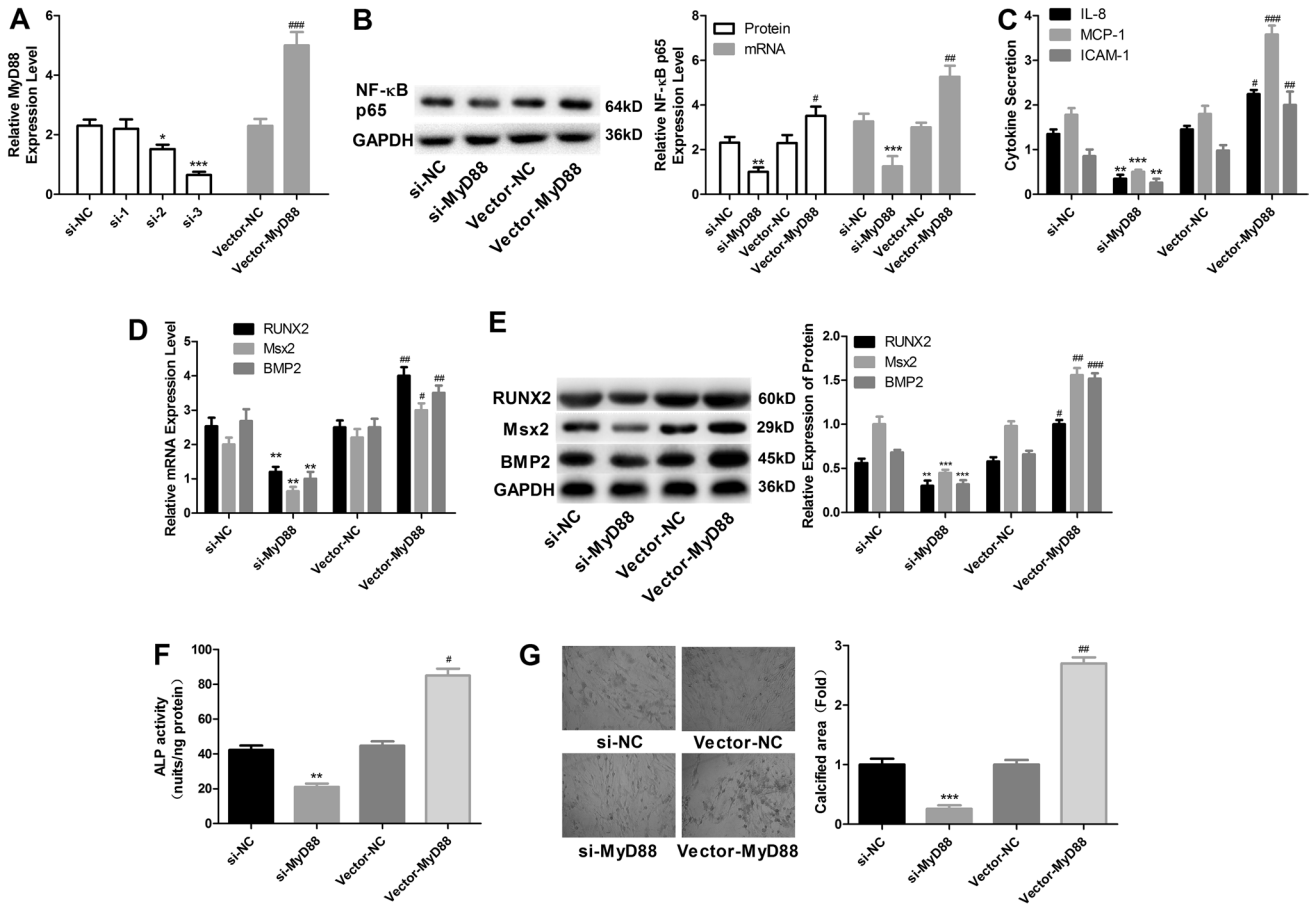

Fig. 5 Determination of the effects of MyD88 on the calcification of AVICs. AVICs were transfected with siRNAs-MyD88, si-RNA-NC, vector-MyD88, and vector-MyD88 to down-regulate and up-regulate MyD88 expression, respectively. **a** RT-PCR was performed to detect the transfected efficiency of siRNAs-MyD88 and vector-MyD88 after 24 h of the transfection. **b** RT-PCR and western blot tests were used to assess the mRNA and protein levels of NF-κB after up-regulation and down-regulation of MyD88 in AVICs. **c** ELISA assay analysis of the protein levels of IL-6, IL-8, and MCP-1 in the supernatant of AVICs after 48 h of the transfection. **d, e** RT-PCR and western blot tests were used to assess the mRNA and protein levels of RUNX2, Msx2, and BMP2 after up-regulation and down-regulation of MyD88 in AVICs. **f** F ALP activity of AVICs after 7 days of cell transfection. G Calcified nodules were apparent by alizarin red staining 48 h after transfection. Magnification: ×100. Error bars represent the mean ± SD of at least three independent experiments. (*$P<0.05$, **$P<0.01$, ***$P<0.001$, si-MyD88 vs si-NC; $^{\#}P<0.05$, $^{\#\#}P<0.01$, $^{\#\#\#}P<0.001$, vector-MyD88 vs vector-NC)

MiR-214 was highly expressed in the blood samples from CAVD patients, and transfection of the miRNA-214 inhibitor into AVICs blocks the osteoblastic transformation. To the best of our knowledge, this is the first report of miR-214 up-regulation in CAVD patients and its involvement in the osteoblastic transformation of AVICs. In bone-marrow mesenchymal stem cells (BMSCs), Li et al. [18] reported that miR-214 was down-regulated, while β-catenin and RUNX2 were enhanced in the process of BMSCs differentiating into osteoblasts; miR-214 agomir significantly declined RUNX2 level and attenuated osteoblast differentiation in BMSCs. Shi et al. [26] found that miR-214 suppressed osteogenic differentiation of C2C12 myoblast cells by targeting osterix. In contrast to these findings, the present study showed that miR-214 was up-regulated in the CAVD patients and promoted the osteogenic differentiation of AVICs, which was consistent with a previous report [27] that demonstrated knockdown of miR-214 in mice seemed to improve aortic valve calcification in apoE$^{-/-}$ mice with high-cholesterol (HC)-diet induced aortic valve calcification..

Besides, we observed that the expression of TLR4, MyD88 and NF-κB were elevated in patients with CAVD when compared with the matched control individuals, suggesting that the elevated TLR4, MyD88, and NF-κB might be involved in the progression of CAVD. Previous study have proved that TLR4 plays a key role in innate and adaptive immunity in the physiological process of CAVD [28]. MyD88, a critical adapter protein for TLR4, leads to the activation of downstream NF-κB and the subsequent production of pro-inflammatory cytokines [29]. Studies have suggested that the NF-κB pathway plays a vital role in modulating TLR4-mediated inflammatory and osteogenic responses

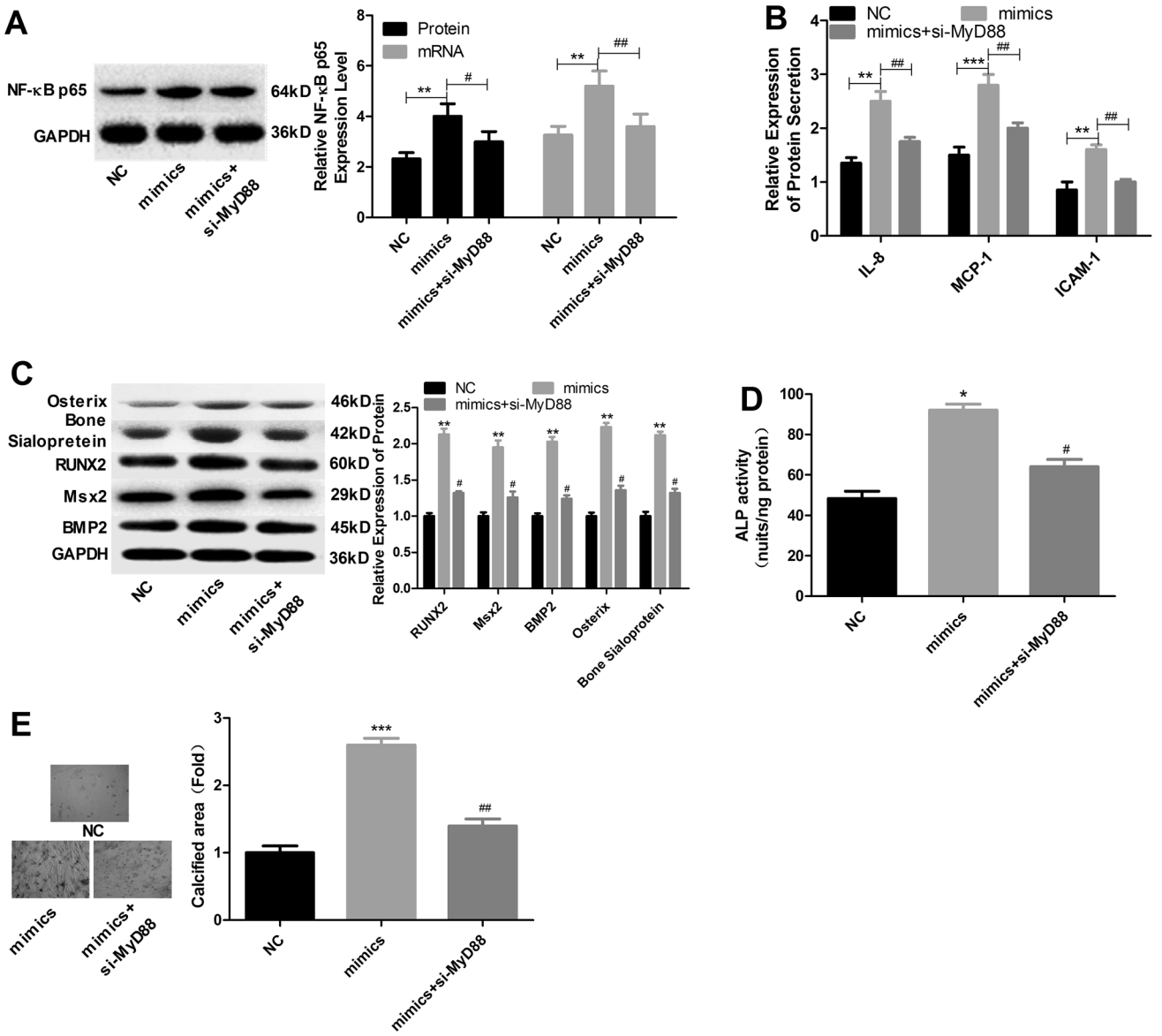

Fig. 6 Analysis of the function of miR-214/MyD88 in the inflammation and calcification of AVICs. **a** Western blot tests were used to assess the mRNA and protein levels of NF-κB after AVICs were given different treatments: NC, mimic-miR-214 and mimic-miR-214 + si-MyD88. **b** ELISA assay analysis of the protein levels of IL-8, MCP-1, and ICAM-1 in the supernatant of AVICs after 48 h of the cells were transfected with NC, mimic-miR-214 and mimic-miR-214 + si-MyD88. **c** Western Blot tests were used to assess the protein expression of osterix, bone sialoprotein, RUNX2, Msx2, and BMP2 48 h after the cells were transfected with NC, mimic-miR-214, and mimic-miR-214 + si-MyD88. **d** ALP activity of AVICs after 7 days of cell transfection. **e** Calcified nodules were apparent by alizarin red staining 48 h after transfection. Magnification: ×100. Error bars represent the mean ± SD of at least three independent experiments. (*$P < 0.05$, **$P < 0.01$, mimic-miR-214 vs NC; $^{\#}P < 0.05$, $^{\#\#}P < 0.01$, mimic-miR-214 + si-MyD88 vs mimic-miR-214)

in human AVICs [10, 30]. Stimulation of TLR4 in human AVICs with LPS not only induces the production of inflammatory mediators, but also up-regulates the expression of osteogenic factors, including BMP-2 and ALP [31]. Similarly, this study demonstrated that LPS promoted the expression of inflammatory responses, with elevated expression of IL-6, IL-8, MCP-1, and ICAM-1. All of these cytokines exert important auxo-action in the inflammatory responses of AVICs [32, 33] and are present in the early aortic valve lesions associated with CAVD [5].

The present study also showed that LPS promoted the expression of IL-6, IL-8, MCP-1, and ICAM-1 regardless of miR-214 was up-regulated or down-regulated, suggesting either that miR-214 and LPS are two independent ways through which inflammatory processes are facilitated in AVICs or that LPS is upstream of miR-214 in the

inflammation pathway [27]. To further explore if the TLR4/MyD88/NF-κB pathway is involved in the inflammatory responses induced by miR-214, we performed RT-PCR and western blot analysis to detect the expression of TLR4, MyD88, and NF-κB after AVICs were transfected with the mimic/inhibitor of miR-214. We found that miR-214 increased the expression of MyD88 and NF-κB, while having no influence in TLR4 expression. However, we did not investigate miR-214 effect on the expression of other TLRs family members in the current study, hence we were inconclusive about deciding if miR-214 accelerated the progression of CAVD in a TLR-independent way. Besides, we found that miR-214 could directly combine with MyD88 protein which has a direct or indirect combination with NF-κB protein, suggesting that MyD88/NF-κB signaling was strongly implicated in the process in which miR-214 accelerated the pathogenesis of CAVD. MyD88-dependent pathway leads to the rapid activation of NF-κB, resulting in the increased secretion of inflammatory mediators in most cell types [34]. Additionally, it has been demonstrated that the MyD88/NF-κB-mediated signaling pathway plays an important role in mediating tissue inflammation in many conditions, including cardiovascular calcification [35]. Similarly, we found that the inhibition of inflammatory and calcific reactions of AVICs induced by miR-214 inhibitor was abolished when MyD88 was up-regulated, suggesting that MyD88 was closely involved in miR-214-mediated inhibition of inflammatory and calcific reactions.

In conclusion, this study showed that miR-214 promoted calcification by facilitating inflammatory reaction through activating MyD88/NF-κB signaling pathway in AVICs, which might provide a new target for CAVD diagnosis and treatment.

Funding This study was funded by the Science Project of Nantong (no. MS 22015077, no. MS 32015027) and Nantong University Teaching Reform Project (no. 2016B93).

Compliance with ethical standards

Conflict of interest The authors declare that they have no competing interests.

References

1. Coffey S, Cox B, Williams MJ (2014) The prevalence, incidence, progression, and risks of aortic valve sclerosis: a systematic review and meta-analysis. J Am Coll Cardiol 63(25 Pt A):2852–2861. https://doi.org/10.1016/j.jacc.2014.04.018
2. Lindman BR, Clavel MA, Mathieu P, Iung B, Lancellotti P, Otto CM, Pibarot P (2016) Calcific aortic stenosis. Nat Rev Dis Primers 2:16006. https://doi.org/10.1038/nrdp.2016.6
3. Hutcheson JD, Aikawa E, Merryman WD (2014) Potential drug targets for calcific aortic valve disease. Nat Rev Cardiol 11(4):218–231. https://doi.org/10.1038/nrcardio.2014.1
4. New SE, Aikawa E (2011) Molecular imaging insights into early inflammatory stages of arterial and aortic valve calcification. Circ Res 108(11):1381–1391. https://doi.org/10.1161/CIRCRESAHA.110.234146
5. Otto CM, Kuusisto J, Reichenbach DD, Gown AM, O'Brien KD (1994) Characterization of the early lesion of 'degenerative' valvular aortic stenosis. Histological and immunohistochemical studies. Circulation 90(2):844–853
6. Cote N, Mahmut A, Bosse Y, Couture C, Page S, Trahan S, Boulanger MC, Fournier D, Pibarot P, Mathieu P (2013) Inflammation is associated with the remodeling of calcific aortic valve disease. Inflammation 36(3):573–581. https://doi.org/10.1007/s10753-012-9579-6
7. Weiss RM, Miller JD, Heistad DD (2013) Fibrocalcific aortic valve disease: opportunity to understand disease mechanisms using mouse models. Circ Res 113(2):209–222. https://doi.org/10.1161/CIRCRESAHA.113.300153
8. Mohler ER 3rd, Chawla MK, Chang AW, Vyavahare N, Levy RJ, Graham L, Gannon FH (1999) Identification and characterization of calcifying valve cells from human and canine aortic valves. J Heart Valve Dis 8(3):254–260
9. Lopez J, Fernandez-Pisonero I, Duenas AI, Maeso P, San Roman JA, Crespo MS, Garcia-Rodriguez C (2012) Viral and bacterial patterns induce TLR-mediated sustained inflammation and calcification in aortic valve interstitial cells. Int J Cardiol 158(1):18–25. https://doi.org/10.1016/j.ijcard.2010.12.089
10. Zeng Q, Jin C, Ao L, Cleveland JC Jr, Song R, Xu D, Fullerton DA, Meng X (2012) Cross-talk between the Toll-like receptor 4 and Notch1 pathways augments the inflammatory response in the interstitial cells of stenotic human aortic valves. Circulation 126(11 Suppl 1):S222–S230. https://doi.org/10.1161/CIRCULATIONAHA.111.083675
11. Yang X, Fullerton DA, Su X, Ao L, Cleveland JC Jr, Meng X (2009) Pro-osteogenic phenotype of human aortic valve interstitial cells is associated with higher levels of Toll-like receptors 2 and 4 and enhanced expression of bone morphogenetic protein 2. J Am Coll Cardiol 53(6):491–500. https://doi.org/10.1016/j.jacc.2008.09.052
12. Yu Z, Seya K, Daitoku K, Motomura S, Fukuda I, Furukawa K (2011) Tumor necrosis factor-alpha accelerates the calcification of human aortic valve interstitial cells obtained from patients with calcific aortic valve stenosis via the BMP2-Dlx5 pathway. J Pharmacol Exp Ther 337(1):16–23. https://doi.org/10.1124/jpet.110.177915
13. Alexopoulos A, Bravou V, Peroukides S, Kaklamanis L, Varakis J, Alexopoulos D, Papadaki H (2010) Bone regulatory factors NFATc1 and osterix in human calcific aortic valves. Int J Cardiol 139(2):142–149. https://doi.org/10.1016/j.ijcard.2008.10.014
14. Berindan-Neagoe I, Monroig Pdel C, Pasculli B, Calin GA (2014) MicroRNAome genome: a treasure for cancer diagnosis and therapy. CA Cancer J Clin 64(5):311–336. https://doi.org/10.3322/caac.21244
15. Pasquinelli AE (2012) MicroRNAs and their targets: recognition, regulation and an emerging reciprocal relationship. Nat Rev Genet 13(4):271–282. https://doi.org/10.1038/nrg3162
16. Ambros V (2003) MicroRNA pathways in flies and worms: growth, death, fat, stress, and timing. Cell 113(6):673–676
17. Fang M, Wang CG, Zheng C, Luo J, Hou S, Liu K, Li X (2017) Mir-29b promotes human aortic valve interstitial cell calcification via inhibiting TGF-beta3 through activation of wnt3/beta-catenin/Smad3 signaling. J Cell Biochem. https://doi.org/10.1002/jcb.26545
18. Li JP, Zhuang HT, Xin MY, Zhou YL (2017) MiR-214 inhibits human mesenchymal stem cells differentiating into osteoblasts through targeting beta-catenin. Eur Rev Med Pharmacol Sci 21(21):4777–4783

19. Messier RH Jr, Bass BL, Aly HM, Jones JL, Domkowski PW, Wallace RB, Hopkins RA (1994) Dual structural and functional phenotypes of the porcine aortic valve interstitial population: characteristics of the leaflet myofibroblast. J Surg Res 57(1):1–21. https://doi.org/10.1006/jsre.1994.1102
20. Meng X, Ao L, Song Y, Babu A, Yang X, Wang M, Weyant MJ, Dinarello CA, Cleveland JC Jr, Fullerton DA (2008) Expression of functional Toll-like receptors 2 and 4 in human aortic valve interstitial cells: potential roles in aortic valve inflammation and stenosis. Am J Physiol Cell Physiol 294(1):C29–C35. https://doi.org/10.1152/ajpcell.00137.2007
21. Mommer L, Wagemaker CA, Ouborg HDEK NJ (2008) Unravelling below-ground plant distributions: a real-time polymerase chain reaction method for quantifying species proportions in mixed root samples. Mol Ecol Resour 8(5):947–953. https://doi.org/10.1111/j.1755-0998.2008.02130.x
22. Ishizeki K, Saito H, Shinagawa T, Fujiwara N, Nawa T (1999) Histochemical and immunohistochemical analysis of the mechanism of calcification of Meckel's cartilage during mandible development in rodents. J Anat 194(Pt 2):265–277
23. Rajamannan NM, Evans FJ, Aikawa E, Grande-Allen KJ, Demer LL, Heistad DD, Simmons CA, Masters KS, Mathieu P, O'Brien KD, Schoen FJ, Towler DA, Yoganathan AP, Otto CM (2011) Calcific aortic valve disease: not simply a degenerative process: a review and agenda for research from the National Heart and Lung and Blood Institute Aortic Stenosis Working Group. Executive summary: calcific aortic valve disease—2011 update. Circulation 124 (16):1783–1791. https://doi.org/10.1161/CIRCULATIONAHA.110.006767
24. Miller JD, Weiss RM, Heistad DD (2011) Calcific aortic valve stenosis: methods, models, and mechanisms. Circ Res 108(11):1392–1412. https://doi.org/10.1161/CIRCRESAHA.110.234138
25. Tsang HG, Cui L, Farquharson C, Corcoran BM, Summers KM, Macrae VE (2018) Exploiting novel valve interstitial cell lines to study calcific aortic valve disease. Mol Med Rep 17(2):2100–2106. https://doi.org/10.3892/mmr.2017.8163
26. Shi K, Lu J, Zhao Y, Wang L, Li J, Qi B, Li H, Ma C (2013) MicroRNA-214 suppresses osteogenic differentiation of C2C12 myoblast cells by targeting osterix. Bone 55(2):487–494. https://doi.org/10.1016/j.bone.2013.04.002
27. Li XF, Wang Y, Zheng DD, Xu HX, Wang T, Pan M, Shi JH, Zhu JH (2016) M1 macrophages promote aortic valve calcification mediated by microRNA-214/TWIST1 pathway in valvular interstitial cells. Am J Transl Res 8(12):5773–5783
28. Song Y, Fullerton DA, Mauchley D, Su X, Ao L, Yang X, Cleveland JC, Meng X (2011) Microfilaments facilitate TLR4-mediated ICAM-1 expression in human aortic valve interstitial cells. J Surg Res 166(1):52–58. https://doi.org/10.1016/j.jss.2009.03.101
29. Li GZ, Zhang Y, Zhao JB, Wu GJ, Su XF, Hang CH (2011) Expression of myeloid differentiation primary response protein 88 (Myd88) in the cerebral cortex after experimental traumatic brain injury in rats. Brain Res 1396:96–104. https://doi.org/10.1016/j.brainres.2011.04.014
30. Zeng Q, Song R, Ao L, Xu D, Venardos N, Fullerton DA, Meng X (2014) Augmented osteogenic responses in human aortic valve cells exposed to oxLDL and TLR4 agonist: a mechanistic role of Notch1 and NF-kappaB interaction. PLoS One 9(5):e95400. https://doi.org/10.1371/journal.pone.0095400
31. Deng X, Meng X, Zeng QC, Fullerton D, Jaggers J (2013) Abstract 15312: the inflammatory and osteogenic responses to Tlr4 stimulation in human aortic valve interstitial cells is greater in adults than children: the role of Stat3 as a negative regulatory mechanism. Circulation 128(22):A15312
32. El Husseini D, Boulanger MC, Mahmut A, Bouchareb R, Laflamme MH, Fournier D, Pibarot P, Bosse Y, Mathieu P (2014) P2Y2 receptor represses IL-6 expression by valve interstitial cells through Akt: implication for calcific aortic valve disease. J Mol Cell Cardiol 72:146–156. https://doi.org/10.1016/j.yjmcc.2014.02.014
33. Song R, Ao L, Zhao KS, Zheng D, Venardos N, Fullerton DA, Meng X (2014) Soluble biglycan induces the production of ICAM-1 and MCP-1 in human aortic valve interstitial cells through TLR2/4 and the ERK1/2 pathway. Inflamm Res 63(9):703–710. https://doi.org/10.1007/s00011-014-0743-3
34. Kaisho T, Akira S (2006) Toll-like receptor function and signaling. J Allergy Clin Immunol 117(5):979–987. https://doi.org/10.1016/j.jaci.2006.02.023 **(quiz 988)**
35. Zhan Q, Zeng Q, Song R, Zhai Y, Xu D, Fullerton DA, Dinarello CA, Meng X (2017) IL-37 suppresses MyD88-mediated inflammatory responses in human aortic valve interstitial cells. Mol Med. https://doi.org/10.2119/molmed.2017.00022